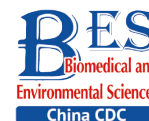# Original Article

Characterization of CircRNA-Associated CeRNA Networks in Folate Deficiency-Induced Neural Tube Defects[*]

WANG Shan[1,2,3,#], ZENG Yu Bing[1], PEI Pei[1], HE Xue Jia[1,2], LIU Fan[1,3], WANG Yi[1], and ZHANG Ting[1,2,3,#]

1. Beijing Municipal Key Laboratory of Child Development and Nutriomics, Capital Institute of Pediatrics, Beijing 100020, China; 2. Capital Institute of Pediatrics-Peking University Teaching Hospital, Beijing 100020, China; 3. Children's Hospital Capital Institute of Pediatrics, Chinese Academy of Medical Sciences & Peking Union Medical College, Beijing 100020, China

Abstract

Objective   Circular RNAs (circRNAs) participate in several important pathological processes and have been used in the diagnosis and treatment of various diseases. This study aimed to investigate the role of circRNAs in neural tube defects (NTDs).

Method   We characterized circRNA-associated competitive endogenous RNA (ceRNA) networks in brain tissue of low folate -induced NTDs mouse at embryonic day 13.5 by high-throughput sequencing. The expression levels of Circzfp644, miR-20-5p and *Gas7* were detected by RT-PCR. *Gas7* and Circzfp644 functions were determined by miRNA-mimics and inhibitors in mouse teratocarcinoma cells (F9 cells), and luciferase gene reporter assay was assessed in the F9 cells. In addition, the expression levels of Circzfp644, miR-20-5p and *Gas7* were determined by Nanostring in human NTDs tissues.

Results   We detected 57 circRNA transcripts, 16 miRNAs, and 148 mRNAs that were significantly dysregulated in NTDs brain tissues compared with their expression levels in control (normal) tissues. Circzfp644 shared miRNA response elements with the growth arrest specific 7 (*Gas7*) gene and competitively bound with miR-20-5p to increase the expression of *Gas7*. Downregulation of Circzfp644 and *Gas7* and upregulation of miR-20-5p were found in human NTD tissue.

Conclusion   This study provides new perspectives on the role of circRNAs in nervous system development and the pathogenesis of NTDs.

Key words: Circzfp644; *Gas7*; miR-20-5p; Folate deficiency; NTDs

INTRODUCTION

During embryonic development, the process of neural tube closure is very sensitive to the external environment, and failure in neural tube closure leads to neural tube malformations[1]. Incomplete neural tube closure, including brain and spinal cord abnormalities, can result in birth defects called neural tube defects (NTDs)[2]. NTDs in craniofacial region result in exencephaly, which could lead to embryonic lethality[3]. Genetics and the environment (e.g., lack of folate or vitamin A) are risk factors of NTDs; however, the mechanisms underlying NTDs in

human remain largely unknown[4]. Some studies stated that fetal neural tube malformed because of the lack of vitamin B12 and folic acid. Vitamin B12 is important for nerve cell metabolism and works with folic acid to promote nervous system development and cell replication. Deficiency of vitamin B12 or folic acid in pregnant women would lead to abnormalities in the development of nervous system, which increases the risk of neural tube abnormalities[5]. Shanxi is a region with high incidence of birth defects in China. Our research group conducted a large number of investigations and studies in this region several years ago, and confirmed that the high rate of birth defects in this region is related to the lack of one-carbon nutrients locally such as folic acid, and the supplementation of folic acid during pregnancy significantly reduces the rate of birth defects[6].

A large number of noncoding RNAs are relevant to nervous system development have been detected by large-scale genome sequencing, including microRNAs (miRNAs) and long noncoding RNAs (lncRNAs)[7]. Unlike linear RNAs have 5' and 3' ends, circular RNAs (circRNAs), are endogenous noncoding RNAs with a closed circular structure without 50→30 polarities and poly (A) tails, and resistant to RNA exonucleases. Most circRNAs are highly stable and cytoplasmic, and many of them are tissue-specific, disease-specific, and timing-specificity[8]. CircRNAs are encoded primarily in exons or introns. There are three main types of cyclization: exonic circRNA, intronic circRNAs, and exon–intron circRNAs, which are formed from back-splicing of exons and/or introns. For cyclization to occur, small nuclear ribonucleoproteins are continuously assembled on the mRNA precursors to catalyze the connection between the downstream 5' donor sites and the upstream 3' acceptor sites. Then, the cord tail is inserted to form a circle, and the circRNA is formed by shearing. Cis-acting regulatory elements promote circRNA formation. CircRNAs have abundant miRNA binding sites and act as miRNA sponges to prevent miRNAs interacting with their target genes and regulating gene expression, in what is called a competing endogenous RNA (ceRNA) network[9]. CircRNA_100290 was shown to function in a ceRNA network to inhibit members of the miR-29 family and regulate the expression of *CDK6*, which prolonged the cell cycle and proliferation[10]. In other studies, circRNA MYLK was found to bind competitively to miRNA-29a-3p, leading to increased expression of its target genes *DNMT3B*, *VEGFA*, and *ITGB1* and the progression of bladder cancer[11]. CircHIPK3 acted as an miR-558 sponge and suppressed heparanase (*HPSE*) expression[12]. In Hirschsprung's

disease, circRNA-ZNF609 was shown to regulate *AKT3* by sponging miR-150-5p in bladder cancer cells.

CircRNAs are known to be involved in many of pathological processes and biological functions, including differentiation, proliferation, apoptosis, development, stress response, disease occurrence, and development[13]. Importantly, some circRNAs are tissue-specific and have stable structures because they do not have accessible terminals and are highly resistant to exonucleases[14]. CircRNAs have been found to have conserved sequences and expression patterns, especially in brain[15]. In mouse and human brain tissues, a circRNA, Cdr1as, that binds specifically to miR-7 and mir-671 was detected. The CRISPR-cas9 genome editing technique was used to selectively eliminate Cdr1as in mice, and the results showed that the expression of most miRNAs was changed in the four studied brain regions[16]. Many circRNAs are highly brain tissue-specific (e.g., specific circRNAs have been found in excitatory neurons[17], and 80% of the circRNAs that were highly expressed in mouse neuron were also detected in human brain. Many of the genes that encode circRNAs are specifically expressed in the brain. When host genes are expressed in other tissues, the proportion of transcripts that encode circRNAs in the brain increases remarkably, suggesting neuro-specific regulation of circRNA production. Genes that carry brain-specific circRNAs, including CircPHF21A, CircirulP4, Circelf2, Circrims2, and circ-MyST4, have key regulatory functions during neuronal and brain development[18]. These results suggest that the circRNA host genes are involved in biological processes relevant to synaptic functions (such as nervous system development, neurogenesis, and neuronal differentiation), including synapses, presynaptic active regions, presynaptic membranes, and postsynaptic density[19]. CircRNA expression profiles were found to change significantly in mouse neural tissues after transient focal ischemia[20].

Environmental factors such as various teratogenic agents, maternal obesity and diabetes, increased oxidative stress may influence neural tube closure (NTC) through a direct effect on metabolic regulation in the context of embryonic development[4]. Deficiency of folates at the cellular level may be responsible in NTDs as a result of disturbed bioavailability of folates. In recent years, a series of RNA-sequencing analyses revealed that circRNAs dynamically expressed in various developmental stages and physiological conditions. It implicated the role of circRNAs in stress response and explored potential mechanisms underlying their regulations.

However, the effects of folate metabolism disorder in the role of circRNAs in neural tube defects (NTDs) remains unclear. In this study, we statistically compared the circRNA expression profiles between NTDs and normal brain tissues in low folate diet and MTX induced NTDs mouse model by high-throughput sequencing. We identified a small number of circRNAs that are up- or down-regulated. These circRNAs may exhibit an important function in NTDs and neural tube development. The results were confirmed in human NTDs fetuses with their maternal blood serum under low folate category, indicating that abnormal expression of Circzfp644 and *Gas7* may disrupt neural development and contribute remarkably to NTDs risk.

MATERIALS AND METHODS

Animals and Establishment of NTDs Mouse Model

C57BL/6 mice were purchased from JinMuYang Ltd aged from 8–10 weeks old, SPF grade. After adaptive feeding for 2 days, mice were fed with low folate diet for 4 weeks. Female mice and male mice were caged overnight at a ratio of 2:1, and the vaginal plug was found in the morning of the second day, which was defined as 0.5 days of gestation. NTDs group (case group) were induced by intraperitoneal injection of methotrexate (MTX) (Sigma, USA) at 1.5 mg/kg body weight on E7.5. The control (con group) group were fed with a normal diet. On E13.5 Embryos, Con (*n* = 3) and NTD (*n* = 3) embryos were dissected and placed in ice- cold tubes, DEPC-treated PBS, respectively. Brain vesicles and spinal cord tissue were isolated from E13.5 d mice, and the samples were divided into three tubes. NTDs Mouse Model were performed as previously mentioned. The details were performed as previously described[21]. All animal experiments were conducted in compliance with the guidelines of the Institute for Laboratory Animal Research, Capital Institute of Pediatrics.

Sample Preparation

Cultured cells and homogenated animal tissues were prepared and total RNA was isolated using TRIzol Reagent (Invitrogen, USA) according to the manufacturer's protocol. RNA was checked directly after extraction by Bioanalyzer 2200 (Aligent) and stored at −80 ℃ until machine analysis. The RNA with integrity number (RIN) > 6.0 is right for rRNA depletion. The RNAs were qualified with RIN > 6.0. The miRNAs were purified by miRNeasy Mini Kit

(Qiagen) and agarose gel electrophoresis was used in the determination.

cDNA Library Construction

Pooled RNA samples were set for the cDNA libraries with the NEBNext® UltraTM Directional RNA Library Prep Kit for Illumina by following the manufacturer's instructions. Samples were fragmented into 150–200 bp after rRNA depletion. The MPure XP Beads (beckman coulter) was used to harvest the target bands. The final cDNA libraries were completed through product purification and enrichment, and then the Illumina HiSeqXTen was used to sequence 150 bp paired-end in a single lane.

miRNA Library Construction and RNA Sequencing

MiRNA library was prepared with total RNA from mice brain. Sample isolation was completed by following to the user's protocol. RNAs were extracted and quantified after purification. The HiSeq 2500 (illumina, USA) was used for library sequenced.

RNA Sequencing Mapping

Clean reads were picked from the raw reads while the adaptor sequences were deleted, the clean reads were then adjusted to mouse genome (version: GRCh38 NCBI) with hisat2. The transcripts were collected to analyze their differential expression in TopHat and Cufflinks[22].

Bioinformatics Analysis and Target Prediction

CircRNA interacts with miRNA like a miRNA sponge and regulate posttranscriptional genes through binding with miRNA recognition elements. We proposed a gene co-expression network to detect gene crosstalk and construct a gene co-expression network based on the normalized signal intensity of specific expressed genes. The pearson correlation was used in every single pair of genes and the most significant correlation pairs were chosen for the network. Degree centrality is significant within a network to measure centrality of a gene. It determines the relative importance. Furthermore, w-cores in graph theory were used instead of graph topology analysis to study certain properties of the networks. The network structure analysis is to determine the relationship between core regulatory factors and its most adjacent genes. They own the biggest differences. Gene ontology illuminated the cellular component, molecular function, and biological process of mRNAs. (GO; http://www.geneontology.org). Kyoto Encyclopedia of Genes and Genomes (KEGG) database was used

for pathway enrichment analysis, annotation and visualization of target genes function.

Cell Culture

Mouse teratocarcinoma cells (F9) were purchased from National Medical Centre of Cell Line Resource. F9 were fed in DMEM with 10% fetal bovine serum (Gibco) and cultured in an incubator containing 5% CO_2 and 37 °C humidified airs.

Western Blot

Proteins were separated in 10% SDS-PAGE. The isolated proteins were transferred from the gel to NC membrane and blocked with 5% skim milk. Incubation with primary antibodies Anti-Gas7 antibody (1:1,000 dilution; Santa Cruz), Anti-GAPDH antibody (1:1,000 dilution; Santa Cruz) overnight at 4 °C, and then incubated with secondary antibody (goat anti-rabbit IgG, 1:2,000, CST, U.S.A.) for 40 min at room temperature.

Cell Transfection

The siRNA targeting against circzfp644 and negative control, as well as mimics of miR-20b-5p were designed and synthesized by GenePharma (Shanghai, China). F9 cells were transfected using Lipofectamine 2000 (Invitrogen) according to the manufacturer's instruction. The designed sequences were shown in Supplementary Table S1 (available in www.besjournal.com).

Luciferase Gene Reporter Assay

F9 cells were cultivated in 24 well plates for transfection. Three UTRs of circrnazfp644 and Gas7 were amplified by PCR, and then subcloned into luciferase reporter vector GP-miRGLO basic. GenePharma (Shanghai, China) Renilla luciferase was used as the control reporter. miR-20-5p mimics or negative controls (100 nm) were transfected with Lipofectamine 2000 (Invitrogen, California, USA) flowing to user's instructions. After 36 hours, the cells were lysed and luciferase activity was detected. The values were normalized to Renilla luciferase transfection control using the dual luciferase reporter gene detection kit (Promega) according to the manufacturer's instructions. The sequences were listed in Supporting Information Supplementary Table S1.

Real-time Q-PCR

Total RNA was extracted using the Trizol reagent (Invitrogen, USA). The RNA to cDNA reverse transcription was performed using Revert Aid First Strand cDNA Synthesis Kit (ABM, Canada). Real-Time PCR was conducted in Quant StudioTM 7 Flex PCR System (Thermo). miRNA was conducted in Hairpin-itTM microRNA and U6 snRNA Normalization RT-PCR Quantitation Kit. The threshold cycle of each sample was recorded, and data were analyzed by normalization to GAPDH values using the $2^{-\Delta\Delta Ct}$ method. U6 was used as an endogenous control gene for miR-20-5p. The primer sequences were listed in Supplementary Table S1.

Human Samples

Clinical samples used in this study included 8 pairs of human NTDs and matched normal tissues were collected from Lvliang area in Shanxi Province with informed consent accepted by patients and their families. The International Classification of Diseases (ICD-10) was used to classify NTDs. Participants were diagnosed by local clinicians. All participates gave written informed consent. The details of surgical procedures are described in other studies[23]. The epidemiological studies are described in detail in our publication[24]. The Ethics Board of Capital Institute of Pediatrics approved the study protocol[6,25].

Nano String nCounter Assay

In this study, NanoString nCounter was used to detect the specific number of transcripts in human NTD fetuses brain tissues. This technology was performed as previously described[26].

Statistical Analysis

Data were analyzed using GraphPad Prism (Version 9.2.0) and SPSS version 19.0 (SPSS Comp., Chicago, IL, USA). All results have been repeated for more than three times. Data were presented as means ± SD. Student's t test or ANOVA analysis was used for group comparisons. When the data did not conform to a normal distribution, nonparametric tests were used. $P < 0.05$ was considered statistically significant and is presented as *$P < 0.05$ or **$P < 0.01$.

RESULTS

CircRNA Profile of Brain Tissue in Low Folate Diets Combined with MTX-induced NTDs

We used mice that were kept under a low folate diet for 4 weeks to construct a mouse model of NTDs by intraperitoneal injection of methotrexate (MTX) (1.5 mg/kg) at embryonic day 7.5 as reported previously[26]. CircRNA transcripts were obtained by high-throughput sequencing analysis of three pairs of normal and NTDs mouse brain tissues.

Hierarchical clustering was performed to visualize the circRNA expression patterns in normal and NTDs mouse brain samples at embryonic day 13.5 (Figure 1A), and the volcano plots showed the variations in circRNA expression levels between the normal and NTDs brain samples (Figure 1B). We found 57 circRNAs that were differentially expressed in the NTDs brain samples compared with their expression in the normal samples; 16 of them were upregulated and 41 were downregulated (Supplementary Table S2, available in www.besjournal.com). To identify important circRNAs associated with NTDs, we constructed gene co-expression networks and predicted the roles of the target genes on the differentially expressed circRNAs by GO-Biology process (BP) analysis (Figure 1C, Supplementary Table S3, available in www.besjournal.com).

Transcriptome Changes in Low Folate Diets Combined with MTX-induced NTDs

Hierarchical clustering was performed to visualize mRNA expression patterns in normal and NTD brain samples (Figure 2A, Supplementary

Table S4, available in www.besjournal.com), and the volcano plots showed the variation in mRNA expression levels between the normal and NTDs brain samples (Figure 2B). We performed Gene ontology (GO) and KEGG pathway enrichment analyses to predict the functions of the target genes (mRNAs). The differentially expressed genes were enriched for multiple GO terms under the three main GO categories, biological process, molecular function, and cellular component. Among them, signaling pathways were highly enriched (Supporting Information Supplementary Figure S1, Supplementary Table S5, available in www. besjournal.com). The enriched KEGG pathways included PI3K-Akt signaling pathway, cGMP-PKG signaling pathway, and protein digestion and absorption. (Figure 2C, Supplementary Table S6, available in www.besjournal.com).

CeRNA Networks Analysis in the NTDs Mouse Brain Tissue

Hierarchical clustering was performed to visualize miRNA expression patterns in normal and NTD brain
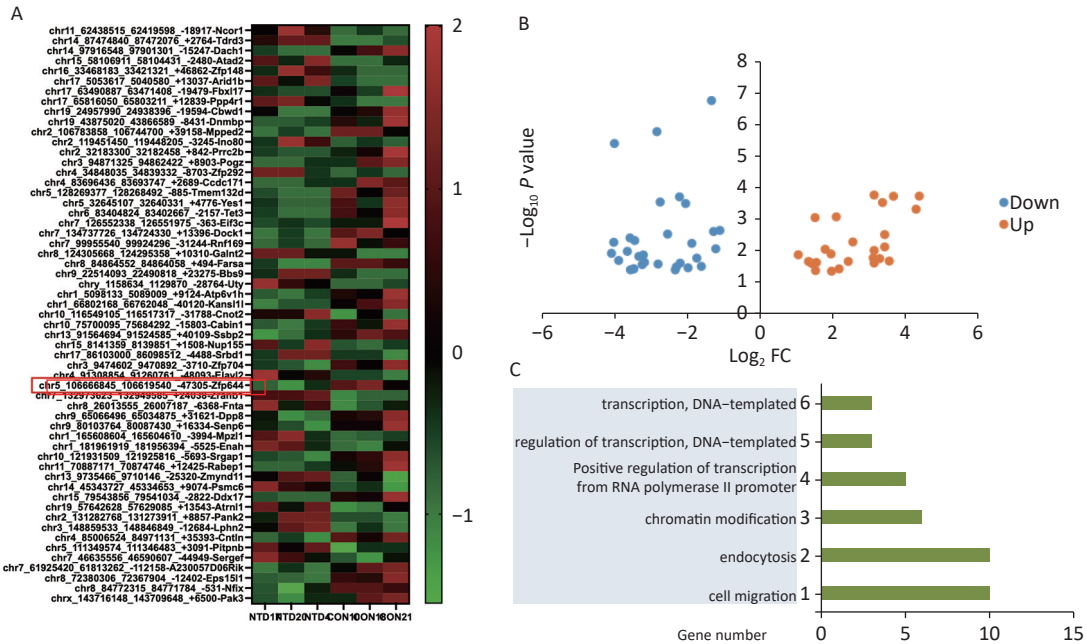

Figure 1. Differentially expressed circRNAs in nervous tissues. (A) Hierarchical cluster analysis of differentially expressed circRNAs in NTDs and normal brain samples; each group includes 3repeats (greater than 1.5-fold changes in expression; $P < 0.05$). Expressions represented in different colors, indicating expression above and below the median across all samples. (B) Volcano plots were constructed in fold-change and p-values. The vertical lines mean 1.5-fold up- or down-regulation in normal and NTDs samples, and the horizontal lines correspond to P-value. The red nodes in the plot represent the differentially expressed circRNAs showing statistical significance. (C) Biology Process (BP) analysis for the host gene dysregulated genes (NTDs *vs.* Con).

samples (Figure 3A, Supplementary Table S7, available in www.besjournal.com), and the volcano plots showed the variation in miRNA expression levels between the normal and NTDs brain samples (Figure 3B). We found 16 miRNAs that were differentially expressed in the NTDs brain samples compared with their expression in the normal samples; 7 of them were upregulated and 9 were downregulated. Overall, miRNA-20-5p had a statistically significant increase in NTDs mouse sample. Consistent with RNA-seq data, RT-qPCR showed that mmu-miR-20b-5p was significantly upregulated in brain and spine of NTDs mouse tissue samples (Figure 3C). Next, we performed ceRNA analysis. On

previously the basis of the analysis strategy, the differentially expressed miRNAs were screened and collected from miRanda (Score ≥ 140 and Energy < −15). The negative correlation between miRNA and circRNA, miRNA and mRNA, miRNA and circRNA was selected[27]. Then 50 circRNA-miRNA- mRNA pathways were constructed, including 5 circRNAs, 12 mRNAs, and 4 miRNAs (Figure 3D). The circRNA-miRNA-mRNA relationships were shown in Supplementary Table S8, available in www.besjournal.

Circzfp644 Targets Gas7 in the NTDs Mouse Brain Tissue

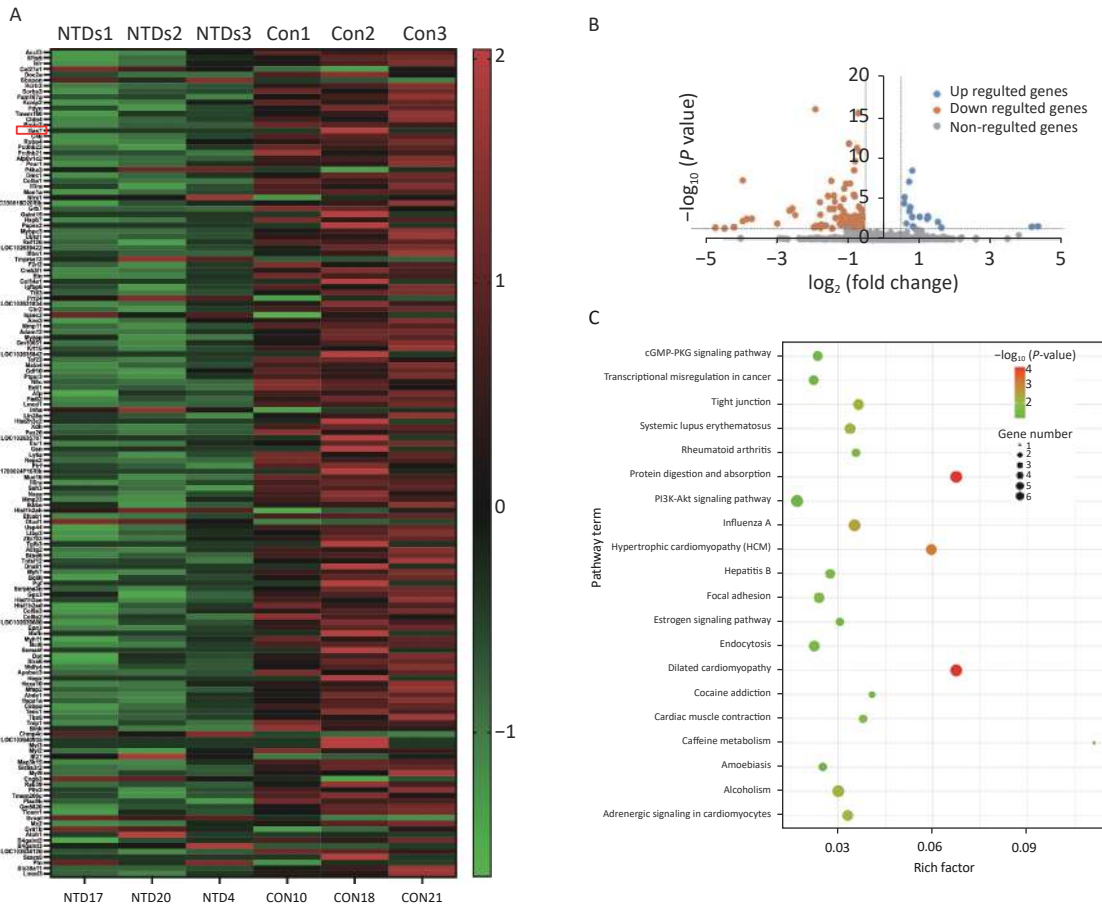The RNA-seq showed that miRNA-20-5p had a

Figure 2. Differential expression and enrichment analysis of mRNA in Neural Tube Defects . (A) cluster analysis of mRNA between NTDs and normal brain samples; each group contains three repeats (greater than 1.5-fold difference in expression; $P < 0.05$). Results are represented in different colors, indicating expression levels above and below the median across all samples. (B) Volcano plots displayed in fold-change and P-values. The vertical lines mean 1.5-fold up- or down-regulation between normal and NTDs samples. and the horizontal line correspond to a P-value. The red-colored point in the plot represents the differentially expressed mRNA with statistical significance. (C) KEGG enrichment of biological process molecular function and cell component of mRNA. The $-\log_{10} P$ value of enrichment is shown on x axis; the numbers represent the number of associated proteins for each term.

statistically significant increase in NTDs sample and RT-qPCR analysis acted consistently with the RNA-seq data. Above our ceRNA analysis, we found that circzfp644 - miRNA-20-5p target on four different mRNAs, *Cngb3*, *Nfic*, *Chmp4c*, *Scara5*, *Cygb* and *Gas7*. *Gas7* is expressed primarily in terminally differentiated brain cells and predominantly in mature cerebellar Purkinje neurons. *GAS7* plays a putative role in neuronal development in human. *Gas7* is involved not only in neurogenesis but also in the regulation of neuronal cell death in murine. *Gas7* is preferentially expressed in the nervous system and participates in the neurogenesis of mammals[28]. To demonstrate the feasibility and value of the constructed ceRNA networks, we chose the circzfp644 - miRNA-20-5p - Gas7 network for further validation. Firstly, we examined the expression level

of *Gas7* and circzfp644 in the NTDs tissue samples. *Gas7* was in one of the top 20 differentially expressed mRNAs (Supporting Information Supplementary Table S4), and found to be significantly downregulated in the NTDs tissue samples by RNA-seq (Figure 2B). Consistent with RNA-seq data, RT-qPCR assays were performed on cranial neural tissue of E13.5 mouse embryos, indicated that the mRNA level of *Gas7* decreased significantly, in NTDs embryos compared to that in controls (Figure 4A). Western blots showed that the Gas7 level was remarkably decreased in cranial neural tissues in E13.5 embryos (Figure 4B). Next, as shown in Figure 4C, Circzfp644 expression was significantly downregulated, which is consistent with the results from the high-throughput sequencing data. We also analyzed that the exon structure of
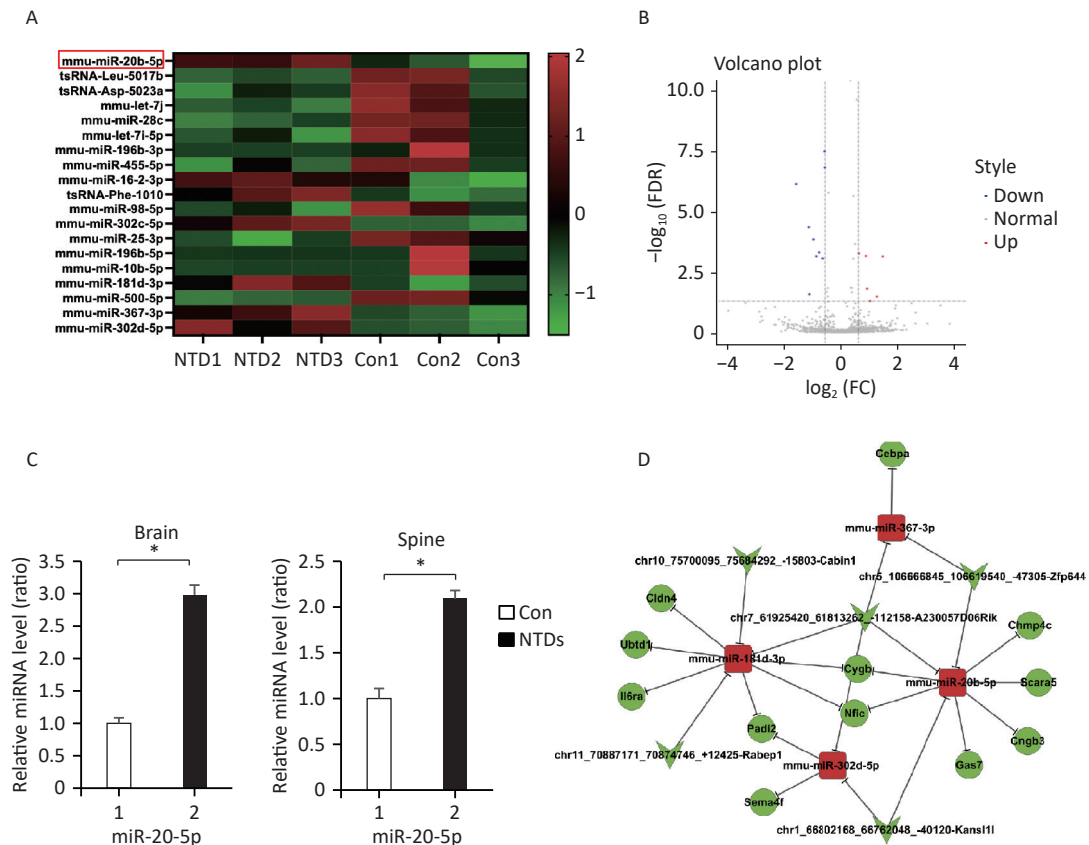
Figure 3. CeRNA networks analysis in the NTD mouse brain tissue. (A) Cluster analysis of small RNA between NTDs and normal brain samples; each group contains 3 individuals (greater than 1.5-fold difference in expression; *P* < 0.05). (B) Volcano plots were constructed using fold-change values and *P*-values. The vertical lines correspond to 1.5-fold up- and down-regulation between normal and NTDs samples. (C) miR-20-5p in cranial neural tissue of mouse NTDs was measured by RT-qPCR. Data are mean ± SD (*n* = 3). (D) circRNAs-miRNAs-mRNAs network consists of 12 genes. In the network, circle represents circRNA and rhombus represents mRNA and inverted triangle represents miRNA, and their relationship was represented by line.

Circzfp644, which is derived from zinc finger protein 644 (zfp644) gene, was 3,539-nt long. The same results found as previously studies[29]. The back-spliced junction of Circzfp644 was amplified by RT-PCR using divergent primers (Supporting Information Supplementary Figure S2, available in www.besjournal.com). To further detect the role of circRNA-zfp644, small interfering RNAs (siRNAs) were constructed and transfected into in F9 cell lines. Both of RT-qPCR and western blots showed that Circzfp644 knockdown significantly reduced the Gas7 levels in F9 cells (Figure 4D and 4E). Together, these results suggest that *Gas7* is the main candidate target of Circzfp644 in the ceRNA networks.

Circzfp644 Relieves the Effect of miR-20-5p on Gas7

CircRNAs function as miRNA sponges to regulate the expression of the target genes[30]. Next, we explored whether Circzfp644 acted as a sponge to regulate *Gas7* expression through the ceRNA networks. The 3' UTR sequence of Circzfp644 complemented the sequences of mmu-miR-20b-5p. We selected miRNAs that were common for Circzfp644 and *Gas7* based on the bioinformatics analysis and preformed AGO2 immunoprecipitation

assays to determine whether Circzfp644 was an intermediate for AGO2 and miR-20-5p. As shown in Figure 5A, Circzfp644 was specifically enriched in miR-20-5p mimic cells. To determine whether Circzfp644 and *Gas7* could be regulated by miR-20-5p, we constructed luciferase reporters containing wild-type and mutated binding sites of Circzfp644 and *Gas7*. The luciferase reporter assays showed that wild-type Circzfp644 and *Gas7* were significantly reduced in miR-20-5p mimics, whereas the mutated Circzfp644 and *Gas7* were not affected compared with the controls (Figure 5B, C). The Q-PCR analyses showed that miR-20-5p mimics significantly decreased both *Gas7* and circRNA-zfp644 levels in F9 cells (Figure 5D, E). The western blot analyses showed that miR-20-5p mimics significantly decreased Gas7 protein levels in F9 cells (Figure 5F). These results suggest that Circzfp644 acts as a sponge for miR-20-5p to regulate *Gas7* expression *via* a ceRNA network.

Circzfp644 and Gas7 Expression Levels are Decreased in Low Folate Mouse NTDs Fetuses

CircRNAs have been shown to be highly enriched in neural tissues of mammals[31-33]. We
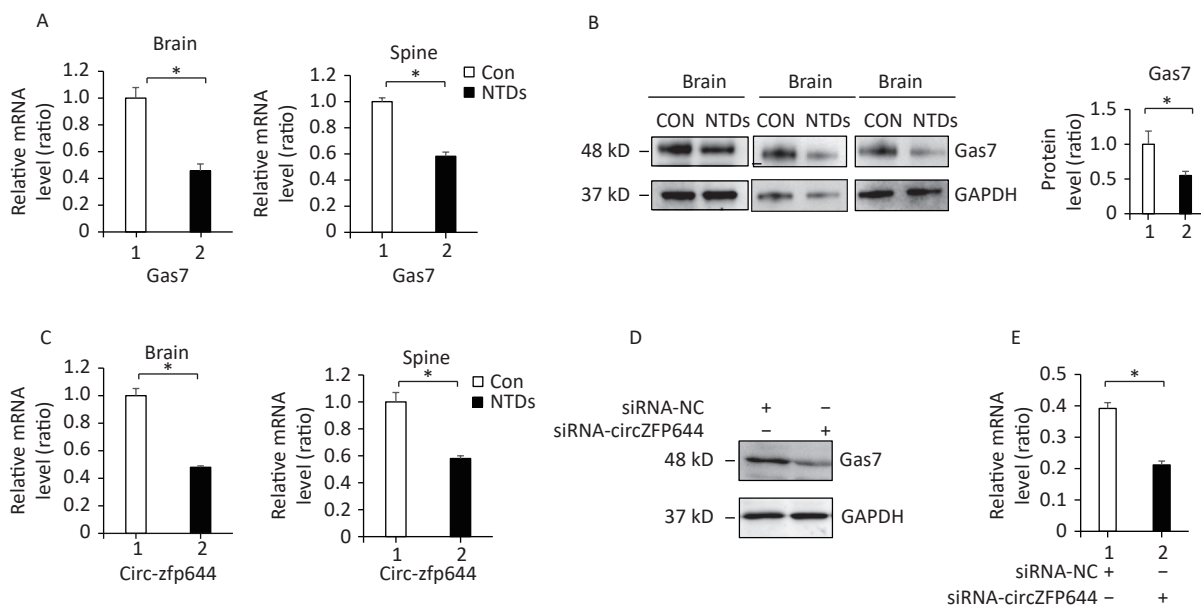
Figure 4. Circzfp644 targets *Gas7* in the NTD mouse brain tissue. (A) *Gas7* mRNA in cranial neural tissue of mouse NTDs was quantified by RT-qPCR. Data are mean ± SD (*n* = 3). (B) Cranial neural tissue of normal and NTDs mouse was achieved at E13.5, and analyzed by western blotting. Aliquots of total lysates were immunoblotted to Gas7 antibody. (C) Expression of circRNAzfp644 was quantified by qPCR. ΔCt was used to measure gene expression normalized against GAPDH expression levels. Normal group = 3, NTDs group = 3. The presented values are the means ± SD. (D, E) mRNA and protein levels of Gas7 in the F9 cells with circzfp644 knockdown.

Figure 5. Circzfp644 sponges with miR-20-5p and inhibits its activity for Gas7 expression. (A) Enrichment of circzfp644 detected through RIP in F9 cells transfected with miR-20-5p mimics or mimics NC. (B) Luciferase reporter assay of circzfp644 and Gas7-3'UTR in F9 cells co-transfected with miR-20-5p mimics or mimics NC. (C) Lucifera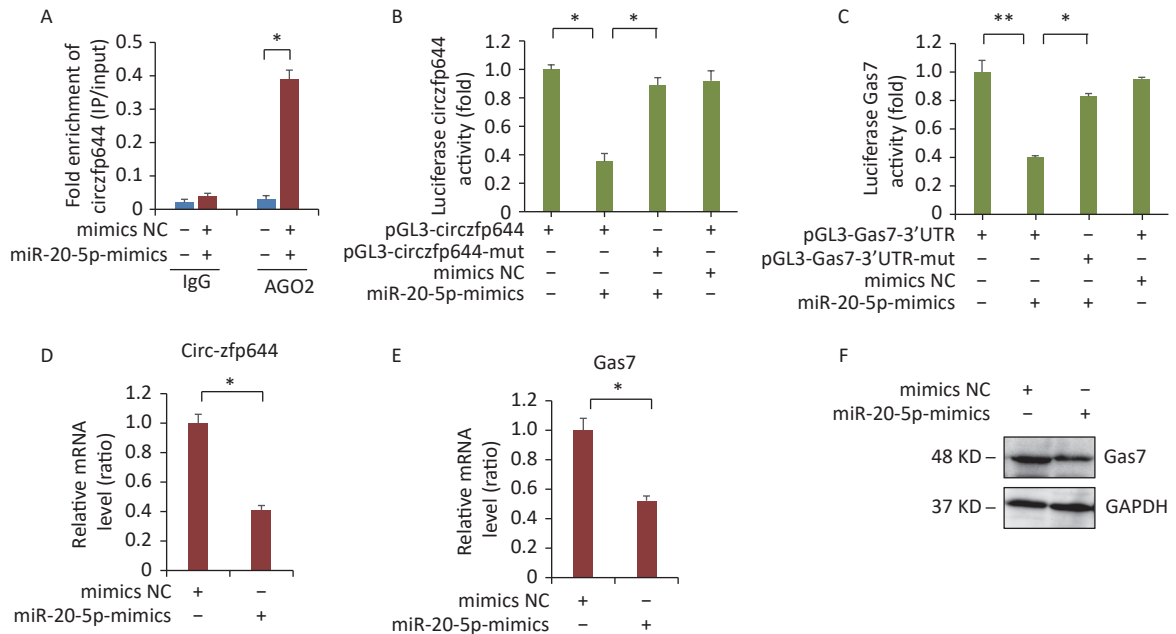se reporter assay of Gas7–3'UTR with circzfp644 knockdown in F9 cells. (D) circzfp644 was measured by RT-qPCR. Data are mean ± SD circzfp644expression in F9 cells transfected with miR-20-5p mimics.(E) *Gas7* mRNA was measured by RT-qPCR. Data are mean ± SD *Gas7* expression in F9 cells transfected with miR-20-5p mimics. (F) Cell lysate was detected Gas7 antibody. F9 cells were transfected with the miR-20-5p mimics or mimics NC.

Table 1. Summary of eight fetus brain and their folate level paired, including fetuses with spina bifida

Sample type	Tissue	Folate level (ng/mg)	Gender	Gestational weeks
Normal	Brain	0.257867	Female	18W
Normal	Brain	0.239733	Female	19W
Normal	Brain	0.241330	Male	18W
Normal	Brain	0.252800	Female	18W
Normal	Brain	0.236670	Male	18W
Normal	Brain	0.158632	Female	14W
Normal	Brain	0.188533	Male	21W
Normal	Brain	0.159184	Male	16W
NTD	Brain	0.056733	Male	21W
NTD	Brain	0.018670	Male	40W
NTD	Brain	0.074600	Female	25W
NTD	Brain	0.064133	Female	25W
NTD	Brain	0.050133	Female	26W
NTD	Brain	0.061867	Male	31W
NTD	Brain	0.065133	Female	34W
NTD	Brain	0.068933	Female	25W

evaluated brain tissue of human NTDs fetuses and the folate levels in the corresponding maternal serum. Eight fetus brain and their folate level paired, including fetuses with spina bifida, with

closely matched age and sex of the fetuses were selected, as summarized in Table 1. Maternal serum folate levels were lower in the pairs with fetuses with spina bifida than in the controls (Figure 6A,

Figure 6. Down-regulated of Circzfp644 and Gas7 expression in low-folate NTDs. (A) Detection of maternal serum folate between normal fetus and NTDs fetus. Data displayed in IQ^R. ($n = 8$), $^*P < 0.05$, by Mann-Whitney U test. (B) The mRNA expression of Circzfp644, *GAS7*, MiR-20-5p in NTDs fetuses' brain, detected by Nanostring. Data displayed in IQ^R. ($n = 8$), $^*P < 0.05$, by Mann-Whitney U test. (C) Detection of Gas7 in brain tissues from normal fetus and NTDs in low folate maternal serum. GAPDH was used as a loading control. Data are mean ± SD. ($n = 3$), $^*P < 0.05$, by Student's t-test.

Supporting Information Supplementary Figure S3A, available in www.besjournal.com). Furthermore, we quantified Cirnzfp644, *Gas7* and miRNA-20-5p expression using NanoString nCounter in brain tissue of fetuses with 8 NTDs patients. We test of normality tests' between the NTD and control groups. However, the results of normality test do not conform to normal distribution. nCounter analysis showed that expression of Cirnzfp644 and *Gas7* expression levels were downregulated in human NTDs fetuses brain samples, whereas miRNA-20-5p expression was upregulated with nonparametric test. (Figure 6B, Supporting Information Supplementary Figure S3B). Western blot analysis of the eight NTDs samples and eight controls with age and sex matched showed that Gas7 levels in most anencephaly samples decreased by 10%–80% (Figure 6C). These results indicated that low folate levels may decrease both *Gas7* and Circzfp644 levels, thereby potentially increasing miRNA-20-5p expression levels, leading to NTDs.

DISCUSSION

NTDs are congenital malformations mainly led by abnormal development of brain and/or spinal cord due to incomplete closure or disorders of segmentation of the neural tube during early embryonic development. Many studies on NTDs have focused on miRNAs and lncRNAs, whereas the role of circRNAs in the occurrence of NTDs is still largely unknown. In this study, whole transcriptome data were systematically analyzed to obtain the expression profiles of circRNAs, miRNAs, and mRNAs in embryonic day 13.5 NTDs mouse brain tissues. On the basis of the co-expression profiling analyses of circRNAs and mRNAs, we identified Circzfp644 as a significantly downregulated circRNA in NTDs tissues. Circzfp644 exerted its function through a ceRNA network by competitively binding to miR-20-5p, which had a suppressive effect on the target gene *Gas7*, implying that Circzfp644 had potential role in the development of NTDs *via* a ceRNA network (Supplementary Figure S4, available in www. besjournal.com).

Exon transcripts can form circRNAs by a back-splicing process. CircRNAs are widely expressed in human cells, and their expression levels can be ≥ 10 times more than their linear isomers[13]. Compared with other noncoding RNAs, such as miRNA and lncRNAs, these characteristic circRNAs are naturally ideal biomarkers and potential therapeutic agents. CircRNAs are highly expressed in human brain,

mouse brain, and rat brain. Examples of brain-specific circRNAs include Circrims2, Circtulp4, Circelf2, Circphf21a, and Circ-myst4, most of which are encoded in genes with key regulatory functions during neuronal and brain development[32]. In this study, we established a low folate diet with MTX-induced mouse NTDs model at E13.5 and found 57 circRNAs that were differentially expressed in the NTDs brain samples compared with the normal samples; 16 of them were upregulated and 41 were downregulated (Figure 1A, B). These dysregulated circRNA may provide new insights into the role of CircRNA in neural development and NTDs occurrence. To our knowledge, this is the first reported study of circRNAs expression profile in NTDs. Our study also found the that low levels of circzfp644 observed in both brain tissue of mouse and human NTD cases in the corresponding NTDs samples with low-folate levels (Figure 4C and Figure 6B). Previously studies found that the circRNAs involved in various stress such as redox homeostasis and metabolism[34]. CircRNAs may function to maintain homeostasis in different stress response to adapt response pathways. Many circRNAs is regulated as a product of increased transcription. circRNAs may play important roles response to stress, such as function on transcription of stress related genes, protecting linear RNAs. Next, we also found that the differentially expressed mRNAs were enriched in KEGG pathways associated with nervous system development (Figure 2C). We explored the downregulation of *Gas7* in brain tissues of fetuses with NTDs that were paired with the corresponding maternal serum folate levels (Figure 6C). These results suggest that folate deficiency may have contributed to the onset of NTDs by altering Circzfp644 levels, thereby affecting the expression of *Gas7*. This sequential regulation of Circzfp644 and *Gas7* may be a potential risk factor for NTDs in response to folate deficiency.

The ceRNA hypothesis states that RNA transcripts such as mRNAs, lncRNAs, and circRNAs share miRNA response elements, compete to bind to miRNAs, and form complex post-transcriptional regulatory networks[35]. We performed bioinformatic analyses to select miRNAs that shared common binding sites with Circzfp644 and *Gas7*. *Gas7* is expressed preferentially in the brain and is involved in morphological differentiation and neurogenesis[36]. In this study, we showed that Circzfp644 upregulated *Gas7* expression (Figure 4D). Then, we constructed Circzfp644 luciferase reporters and found that miR-20-5p reduced the luciferase activity

of the Circzfp644 luciferase reporter (Figure 5B). These results showed that the strongest binding was between Circzfp644 and miR-20-5p, which confirmed that miR-20-5p was the binding target of Circzfp644 (Figure 5B and 5D). We also showed that *Gas7* mRNA was the direct target of miR-20-5p (Figure 5C, 5E and 5F). Circzfp644 has been validated as a sponge of miR-93-5p, and was shown to function in a ceRNA network to upregulate *Limk1* expression by sequestering miR-93-5p in angiotensin II-treated cardiomyocytes[37]. CircZFP644 was found to be negatively correlated with miR-21-3p in Severe acute pancreatitis (SAP)[29]. Together, these results indicate that miR-20-5p can bind with both Circzfp644 and *Gas7*.

Many studies have shown that overexpression of a miRNA in different cell environments can activate nerve cell differentiation. For example, miR-124 may be the best example of a miRNA that controls the fate of nerve cells[38], and miR-20 was found to play a significant role in post-transcriptional regulation of cell proliferation and induced cardiomyocyte hypertrophy[39]. However, the roles of miR-20-5p in NTDs remain unclear. The abundance of miR-20-5p was higher both in the mouse and fetal NTD brain tissues (Figure 3C and Figure 6B). The RNA immunoprecipitation assays confirmed the binding of Circzfp644 to miR-20-5p (Figure 5A), resulting in less miR-20-5p to target *Gas7*. Previous findings have shown that miR-362-5p promotes cell proliferation and cell cycle progression by targeting *GAS7* in acute myeloid leukemia[40]. The identification of a Circzfp644–miR-20-5p–Gas7 ceRNA axis in this study expands the understanding of the underlying mechanism of the progression of NTDs. A number of studies have demonstrated that ncRNAs are important regulators of human brain function. In brain development, some specific miRNAs function on neurons, cerebral cortex, and dendritic branching. Some studies showed that circRNA is differentially expressed in different brain regions, which suggest its potential role in brain development[19]. However, due to the more complexity of human brain function, our research will investigate the interaction between miRNA and circRNA, and the molecular mechanism of transcription factors regulation and chromatin-modifying enzymes in future.

In this study, we found that dysregulated circRNAs identified candidate circRNAs associated with NTDs. Furthermore, we have shown that Circzfp644 competitively binds to miR-20-5p to inhibit its suppressive effect on *Gas7* expression.

These findings link the abnormal expression of Circzfp644 and *Gas7* to the development of NTDs under low-folate conditions, and contribute to the understanding of nervous system development and indicate a potential approach for the diagnosis and treatment of NTDs.

AUTHOR'S CONTRIBUTIONS

SW conceived and designed this study. SW, YZ, and PP participated in laboratory work. SW, YZ, FL, and XH performed the data analysis. SW and YW participated in the writing of the manuscript. SW and TZ participated in advising and revising the manuscript critically. All authors read and approved the final manuscript.

CONFLICTS OF INTEREST

The authors declare that they are no conflict of interests.

ETHICAL APPROVAL

The study was conducted according to the guidelines of the management and utility of experimental animals, and approved by the Ethics Committee of Capital Institute of Pediatrics, Beijing and all animal manipulations were strictly performed following the relevant laws of China. (SHERLLM2021024, DWLL2021011).

REFERENCES

1. Greene NDE, Copp AJ. Neural tube defects. Annu Rev Neurosci, 2014; 37, 221–42.
2. Marean A, Graf A, Zhang Y, et al. Folic acid supplementation can adversely affect murine neural tube closure and embryonic survival. Hum Mol Genet, 2011; 20, 3678–83.
3. Stover PJ. One-carbon metabolism-genome interactions in folate-associated pathologies. J Nutr, 2009; 139, 2402–5.
4. Copp AJ, De Greene N. Genetics and development of neural tube defects. J Pathol, 2010; 220, 217–30.
5. Mason JB, Choi SW, Liu ZH. Other one-carbon micronutrients and age modulate the effects of folate on colorectal carcinogenesis. Nutr Rev, 2008; 66, S15–7.
6. Zhang T, Xin RL, Gu X, et al. Maternal serum vitamin B$_{12}$, folate and homocysteine and the risk of neural tube defects in the offspring in a high-risk area of China. Public Health Nutr, 2009; 12, 680–6.
7. Cech TR, Steitz JA. The noncoding RNA revolution-trashing old rules to forge new ones. Cell, 2014; 157, 77–94.
8. Chen LL, Yang L. Regulation of circRNA biogenesis. RNA Biol, 2015; 12, 381–8.

9. Tay Y, Rinn J, Pandolfi PP. The multilayered complexity of ceRNA crosstalk and competition. Nature, 2014; 505, 344–52.

10. Chen L, Zhang S, Wu J, et al. circRNA_100290 plays a role in oral cancer by functioning as a sponge of the miR-29 family. Oncogene, 2017; 36, 4551–61.

11. Huang MG, Zhong ZY, Lv MX, et al. Comprehensive analysis of differentially expressed profiles of lncRNAs and circRNAs with associated co-expression and ceRNA networks in bladder carcinoma. Oncotarget, 2016; 7, 47186–200.

12. Li YW, Zheng FX, Xiao XY, et al. CircHIPK3 sponges miR-558 to suppress heparanase expression in bladder cancer cells. EMBO Rep, 2017; 18, 1646–59.

13. Zhu KP, Ma XL, Zhang CL. LncRNA FENDRR sensitizes doxorubicin-resistance of osteosarcoma cells through down-regulating ABCB1 and ABCC1. Oncotarget, 2017; 8, 71881–93.

14. Memczak S, Jens M, Elefsinioti A, et al. Circular RNAs are a large class of animal RNAs with regulatory potency. Nature, 2013; 495, 333–8.

15. Ashwal-Fluss R, Meyer M, Pamudurti NR, et al. circRNA biogenesis competes with pre-mRNA splicing. Mol Cell, 2014; 56, 55–66.

16. Fragkouli A, Doxakis E. miR-7 and miR-153 protect neurons against MPP$^+$-induced cell death via upregulation of mTOR pathway. Front Cell Neurosci, 2014; 8, 182.

17. Guo JU, Agarwal V, Guo HL, et al. Expanded identification and characterization of mammalian circular RNAs. Genome Biol, 2014; 15, 409.

18. You XT, Vlatkovic I, Babic A, et al. Neural circular RNAs are derived from synaptic genes and regulated by development and plasticity. Nat Neurosci, 2015; 18, 603–10.

19. Jeck WR, Sorrentino JA, Wang K, et al. Circular RNAs are abundant, conserved, and associated with ALU repeats. RNA, 2013; 19, 141–57.

20. Lin SP, Ye S, Long YM, et al. Circular RNA expression alterations are involved in OGD/R-induced neuron injury. Biochem Biophys Res Commun, 2016; 471, 52–6.

21. MRC Vitamin Study Research Group. Prevention of neural tube defects: results of the Medical Research Council Vitamin Study. Lancet, 1991; 338, 131–7.

22. Zhong YJ, Wang YX, Zhang C, et al. Identification of long non-coding RNA and circular RNA in mice after intra-tracheal instillation with fine particulate matter. Chemosphere, 2019; 235, 519–26.

23. Chen XL, Shen YP, Gao YH, et al. Detection of copy number variants reveals association of cilia genes with neural tube defects. PLoS One, 2013; 8, e54492.

24. Chen XL, Guo J, Lei YP, et al. Global DNA hypomethylation is associated with NTD-affected pregnancy: a case-control study. Birth Defects Res A Clin Mol Teratol, 2010; 88, 575–81.

25. Wang L, Wang F, Guan J, et al. Relation between hypomethylation of long interspersed nucleotide elements and risk of neural tube defects. Am J Clin Nutr, 2010; 91, 1359–67.

26. Pei P, Cheng XY, Yu J, et al. Folate deficiency induced H2A ubiquitination to lead to downregulated expression of genes involved in neural tube defects. Epigenetics Chromatin, 2019; 12, 69.

27. Zhu KP, Zhang CL, Ma XL, et al. Analyzing the interactions of mRNAs and ncRNAs to predict competing endogenous RNA networks in osteosarcoma chemo-resistance. Mol Ther, 2019; 27, 518–30.

28. Hung FC, Cheng YC, Sun NK, et al. Identification and functional characterization of zebrafish Gas7 gene in early development. J Neurosci Res, 2013; 91, 51–61.

29. Yang Y, Ren JD, Huang QL, et al. CircRNA expression profiles and the potential role of CircZFP644 in mice with severe acute pancreatitis via sponging miR-21-3p. Front Genet, 2020; 11, 206.

30. Salmena L, Poliseno L, Tay Y, et al. A ceRNA hypothesis: the Rosetta Stone of a hidden RNA language? Cell, 2011; 146, 353-8.

31. Hombach S, Kretz M. Non-coding RNAs: classification, biology and functioning. Adv Exp Med Biol, 2016; 937, 3–17.

32. Rybak-Wolf A, Stottmeister C, Glažar P, et al. Circular RNAs in the mammalian brain are highly abundant, conserved, and dynamically expressed. Mol Cell, 2015; 58, 870–85.

33. Chen W, Schuman E. Circular RNAs in brain and other tissues: a functional enigma. Trends Neurosci, 2016; 39, 597–604.

34. Zuo JH, Wang Q, Zhu BZ, et al. Deciphering the roles of circRNAs on chilling injury in tomato. Biochem Biophys Res Commun, 2016; 479, 132–8.

35. Liu CY, Zhang CC, Yang J, et al. Screening circular RNA expression patterns following focal cerebral ischemia in mice. Oncotarget, 2017; 8, 86535–47.

36. Bhupana JN, Huang BT, Liou GG, et al. Gas7 knockout affects PINK1 expression and mitochondrial dynamics in mouse cortical neurons. FASEB BioAdv, 2020; 2, 166–81.

37. Chen YQ, Song DF, Gao JX, et al. Circ-Zfp644 acts as a pro-hypertrophic mediator in an Ang-II induced in vitro myocardial hypertrophy model. Cell Biol Int, 2021; 45, 1260–8.

38. Zhu HF, Wang JH, Shao YL, et al. Catalpol may improve axonal growth via regulating miR-124 regulated PI3K/AKT/mTOR pathway in neurons after ischemia. Ann Transl Med, 2019; 7, 306.

39. Wu FQ, Yin CX, Qi JH, et al. miR-362-5p promotes cell proliferation and cell cycle progression by targeting GAS7 in acute myeloid leukemia. Hum Cell, 2020; 33, 405–15.

40. Ali A, Mahla SB, Reza V, et al. Predicting the possible effect of miR-203a-3p and miR-29a-3p on DNMT3B and GAS7 genes expression. J Integr Bioinform, 2021; 19, 20210016.